

Gold Nanoparticles-Based Colorimetric Discrimination of Cancer-Related Point Mutations with Picomolar Sensitivity

Paola Valentini, Roberto Fiammengo, Stefania Sabella, Manuela Gariboldi, gabriele maiorano, Roberto Cingolani, and Pier Paolo Pompa

ACS Nano, **Just Accepted Manuscript** • DOI: 10.1021/nn401757w • Publication Date (Web): 22 May 2013

Downloaded from <http://pubs.acs.org> on May 24, 2013

Just Accepted

“Just Accepted” manuscripts have been peer-reviewed and accepted for publication. They are posted online prior to technical editing, formatting for publication and author proofing. The American Chemical Society provides “Just Accepted” as a free service to the research community to expedite the dissemination of scientific material as soon as possible after acceptance. “Just Accepted” manuscripts appear in full in PDF format accompanied by an HTML abstract. “Just Accepted” manuscripts have been fully peer reviewed, but should not be considered the official version of record. They are accessible to all readers and citable by the Digital Object Identifier (DOI®). “Just Accepted” is an optional service offered to authors. Therefore, the “Just Accepted” Web site may not include all articles that will be published in the journal. After a manuscript is technically edited and formatted, it will be removed from the “Just Accepted” Web site and published as an ASAP article. Note that technical editing may introduce minor changes to the manuscript text and/or graphics which could affect content, and all legal disclaimers and ethical guidelines that apply to the journal pertain. ACS cannot be held responsible for errors or consequences arising from the use of information contained in these “Just Accepted” manuscripts.



1
2
3
4
5
6
7
8
9

Gold Nanoparticles-Based Colorimetric Discrimination of Cancer- Related Point Mutations with Picomolar Sensitivity

10 Paola Valentini¹, Roberto Fiammengo¹, Stefania Sabella¹, Manuela Gariboldi^{2,3}, Gabriele
11
12
13
14
15
16
17
18
19
20
21
22
23
24
25
26
27
28
29
30
31
32
33
34
35
36
37
38
39

Maiorano¹, Roberto Cingolani⁴, and Pier Paolo Pompa^{1*}

1) *Istituto Italiano di Tecnologia, Center for Bio-Molecular Nanotechnologies@UniLe, Via Barsanti –
73010 Arnesano (Lecce), Italy*

2) *Department of Experimental Oncology and Molecular Medicine, Fondazione IRCCS Istituto Nazionale
dei Tumori, Milano, Italy*

3) *Fondazione Istituto FIRC Oncologia Molecolare (IFOM), Milano, Italy*

4) *Istituto Italiano di Tecnologia, Via Morego, 30 – 16136 Genova, Italy*

40 * Corresponding author:

41 Pier Paolo Pompa

42 Center for Bio-Molecular Nanotechnology

43 Italian Institute of Technology (IIT)

44 Via Barsanti - 73010 Arnesano (Lecce), Italy

45 tel: +39-0832- 1816214

46 Fax: +39-0832- 1816230

47 e-mail: pierpaolo.pompa@iit.it

ABSTRACT

Point mutations in the Kirsten rat sarcoma viral oncogene homolog (KRAS) gene are being increasingly recognized as important diagnostic and prognostic markers in cancer. In this work, we describe a rapid and low-cost method for the naked-eye detection of cancer-related point mutations in KRAS, based on gold nanoparticles. This simple colorimetric assay is sensitive (limit of detection in the low picomolar range), instrument-free, and employs non-stringent room temperature conditions, thanks to a combination of DNA-conjugated gold nanoparticles, a probe design which exploits cooperative hybridization for increased binding affinity, and signal enhancement on the surface of magnetic beads. Additionally, the scheme is suitable for point-of-care applications, as it combines naked-eye detection, small sample volumes, and isothermal (PCR-free) amplification.

Keywords: (Biosensors, Colorimetric, Genotyping, Gold Nanoparticles, Stacking interactions)

1
2
3 Point mutations in codons 12 and 13 of KRAS are very common in different types of cancers
4 and have been widely shown to be associated to a poor prognosis. It has been estimated that 17-
5 25% of all cancers harbor mutations in this gene:¹ in particular, these are present in 90% of all
6 pancreas cancers, 33% of non-small cell lung cancer (NSCLC)² and c.a. 40% of metastatic
7 colorectal cancers (mCRC).³ Two mutations at codon 12 of the gene (35G>A and 35G>T) account
8 together for 58% of all KRAS mutations found in cancer.³ In mCRC the presence of these KRAS
9 mutations has also been associated with more aggressive metastatic behavior⁴ and failure to
10 respond to antibody therapies (cetuximab and panitumumab) targeting the Epithelial Growth
11 Factor Receptor (EGFR).¹ Determination of KRAS mutation status is, thus, of crucial importance
12 for therapeutic decisions in the treatment of metastatic colon cancer. In 2009, the American
13 Society of Clinical Oncology (ASCO) stated a provisional clinical opinion, asserting that KRAS
14 mutation testing should be mandatory for all patients with metastatic colon cancer, before
15 undergoing EGFR antibody therapy.⁵ Currently, 12 KRAS mutation test kits, which conform to the
16 requirements of the EU IVD Directive 98/79/EC, are available as diagnostic tools on the European
17 market.⁶ These tests can be distinguished in three categories, based on their underlying working
18 principle, namely real-time PCR, DNA hybridization, or sequencing.⁶ However, the major
19 limitation to large scale utilization of these kits is their elevated cost per sample and the
20 requirement for expensive instrumentation. Therefore, a device allowing cost-effective, rapid and
21 large scale KRAS mutation screening may be very attractive for personalized therapy of cancer
22 patients. Detection of point mutations in human genomic DNA with simple methodologies is quite
23 challenging.⁷ Typically, it is necessary to include in the assay one or more key steps that may
24 increase the number of variables affecting the final result and reduce assay simplicity; this may
25 occur, for instance, when enzymatic reactions,⁸⁻¹⁰ hairpin probes,⁹ additional separation and
26 cleaning steps or melting curve analyses^{10,11} are employed.

1
2
3 In this work, we demonstrated colorimetric detection of the cancer-related point mutation
4 35G>A in KRAS, thanks to the use of gold nanoparticles (AuNPs) combined with signal
5 enhancement on the surface of paramagnetic microparticles. AuNPs are increasingly used as
6 biosensing elements thanks to their interesting optical properties.¹²⁻¹⁷ In particular, they have been
7 used in several colorimetric detection schemes, generally exploiting their color change upon
8 aggregation.¹⁸⁻²⁵ Here, a sensitive and rapid discrimination of the single mismatch under non
9 stringent salt conditions and at room temperature was obtained, thanks to the combination of three
10 factors: *i*) the enhancement of the binding affinities due to cooperative hybridization of
11 oligonucleotides;^{26,27} *ii*) the sharp melting transitions characterizing AuNP-conjugated DNA
12 probes;^{18,28} *iii*) the relatively large nanoparticle size (40 nm), which renders the assay very
13 sensitive, allowing for naked-eye detection. This simple, cost effective and instrument-free
14 detection scheme is suitable for point-of-care (POC) devices. In view of the development of such
15 platforms, we chose, for the target amplification step, the Helicase Dependent isothermal
16 Amplification (HDA),²⁹ which permitted us to avoid the complexity of thermal cycles associated to
17 traditional PCR, while maintaining an amplification efficiency comparable to the latter.
18
19
20
21
22
23
24
25
26
27
28
29
30
31
32
33
34
35
36
37
38
39
40

41 RESULTS

42 Isothermal amplification of KRAS

43
44
45 A KRAS fragment of 101 base pairs was amplified from genomic DNA extracted from HT29
46 wild type (wt) or LS180 mutant (mut) cell lines by means of Helicase Dependent isothermal
47 Amplification (HDA). This technique utilizes a DNA Helicase and single-stranded DNA binding
48 proteins (ssBPs) in order to open the double helix, thus avoiding the need for thermal denaturation
49 of the template.²⁹ The amplification efficiency of the isothermal reaction was similar to a
50 traditional PCR. No unspecific amplification was observed (**Figure 1**). The amplification was
51
52
53
54
55
56
57
58
59
60

1
2
3 obtained at 65 ± 2 °C, suggesting that the reaction well tolerates slight changes in temperature. This
4
5 is a favorable aspect for potential applications of this assay in point-of-care devices, relying on
6
7 simple instrumentation and not requiring complex thermal cycles.
8
9

10 **Colorimetric discrimination of point mutations in KRAS**

11
12 **Figure 2** describes the reaction scheme adopted in this study. The isothermally amplified
13
14 KRAS fragment incorporates one biotin molecule (through the reverse primer), so that it can be
15
16 captured by the streptavidinated paramagnetic microparticles. As the PCR product is double
17
18 stranded, the interfering complementary strand has to be displaced, which is obtained by
19
20 incubation and washing in basic environment. Then, the discriminating probe (**Table 1**) can bind to
21
22 the biotinylated single strand with its 5' portion, and binds the AuNP-conjugated detection probe
23
24 (poly(T)) with its 3' poly(A) tail. During the hybridization, both the mixture containing the
25
26 perfectly matched probe and target and the mixture containing single mismatched pairs appear red.
27
28 The non-hybridized AuNP probes are then removed by magnetic separation. Already after the first
29
30 washing step, the sample containing a single mismatch between the probe and the target starts
31
32 losing its red color and exhibits a yellow background at the end of the third washing step. Notably,
33
34 this naked-eye discrimination of a single point mutation can be achieved under non-stringent salt
35
36 conditions, at room temperature and in about 90 minutes. **Figure 3** shows the visual colorimetric
37
38 detection of point mutation 35G>A in amplified KRAS target and the relative instrumental
39
40 characterization. When KRAS amplified from the homozygous wt cell line HT29 is used,
41
42 hybridization with the perfectly matched wt probe results in an intense red coloration of the
43
44 magnetic beads, due to sandwich hybridization of AuNPs-DNA probes. When the same target is
45
46 tested with the probe specific for the 35G>A mutation, the color of the beads remains yellow,
47
48 indicating that the AuNP-probes, in the presence of a single mismatch, are not retained onto the
49
50 beads surface after magnetic washing (Figure 3A). Interestingly, when KRAS is amplified from
51
52
53
54
55
56
57
58
59
60

1
2
3 the cell line LS180, heterozygous for the 35G>A mutation, an intermediate orange color is
4 observable upon hybridizing the target with either the wt or the 35G>A mut discriminating probes
5 (Figure 3B). A heterozygous cell line can, thus, be distinguished from a homozygous wt or a
6 mutant cell line, which will give a positive signal (red) only with the matched probe. UV-vis
7 spectra of the matched and mismatched samples confirmed the naked-eye inspection, showing a
8 considerable red shift of the absorbance of the beads upon target-induced binding of the AuNP
9 probes. A calibration curve derived from the UV-vis spectra is shown in Supporting Information
10 (Figure S1). The differential spectrum (matched minus mismatched sample) is consistent with the
11 plasmon absorption of AuNPs (Figure 3C). ICP-AES analysis indicates that the gold/iron ratio in
12 samples containing a wt copy of KRAS hybridized with a perfectly matched probe is considerably
13 higher than in samples with a single mismatch (Figure 3D), confirming that the red color observed
14 in the first case is actually due to the AuNPs. Finally, SEM (Figure 3E and 3F) and TEM images
15 (Figure 3G) clearly show a large number of AuNPs decorating the surface of the paramagnetic
16 beads in samples containing the perfectly matched target and probe pairs, unlike samples with a
17 single mismatch. The assay was comparably efficient when using targets amplified by traditional
18 PCR or Helicase Dependent isothermal Amplification (Supporting Information, Figure S2).
19 Notably, the amount of isothermally amplified product necessary for the reaction was as low as 3
20 μ l, without additional purification or processing steps. Working with small volumes of samples is
21 important in view of point-of-care lab-on-chip applications. In order to assess the sensitivity of the
22 method, the amplified target was first quantified by UV spectrophotometry, after purification by
23 polyacrilamide gel electrophoresis, in order to eliminate the non-elongated primers, which could
24 interfere with UV quantification. Then, 32 fmol of amplified target were incubated with the
25 streptavidinated beads at various concentrations, ranging from 1 nM to 10 pM. A clear red color
26 (thus, a naked-eye discrimination of the point mutation) was observed in the presence of the
27
28
29
30
31
32
33
34
35
36
37
38
39
40
41
42
43
44
45
46
47
48
49
50
51
52
53
54
55
56
57
58
59
60

1
2
3 perfect match, down to a target concentration as low as 20 pM (Supporting Information, **Figure**
4
5 **S3**).
6

7 8 **Effect of cooperative hybridization of oligonucleotides and AuNP probes** 9

10 As shown in Figure 2, in our strategy, the AuNP-conjugated detection probe and the target
11 bind to adjacent positions on the discriminating probe molecule. This design allows us to exploit
12 the enhancement in binding affinities due to base pair stacking interactions.^{26,27} To assess whether
13 cooperative hybridization of oligonucleotides was indeed affecting the stability of the final target-
14 probe complex and the assay readout, parallel cooperative binding of the two probes was compared
15 to sequential non-cooperative binding of the same probes. When the discriminating probe and the
16 detection probe were allowed to hybridize at the same time with the target (for a total hybridization
17 time of 70'), a clear colorimetric discrimination of a single mismatch was obtained (**Figure 4**). On
18 the other side, if the two probes were hybridized sequentially, introducing a washing step between
19 the first and the second hybridization, the colorimetric discrimination of the single mismatch was
20 considerably less evident (although the total hybridization time was doubled). This suggests that
21 this short 15 nucleotides (nt) discriminating probe, under the assay conditions, did not stably bind
22 even a perfectly matched target and was largely rinsed away during the washing step. On the
23 contrary, cooperative interactions between the two probes hybridizing at the same time with the
24 target strongly stabilize the binding. Therefore, point mutation discrimination could be achieved at
25 room temperature and under non stringent salt conditions, thanks to the combination of enhanced
26 binding affinity promoted by cooperative hybridization of oligonucleotides, and sharp melting
27 transitions associated to AuNP-probes.
28
29
30
31
32
33
34
35
36
37
38
39
40
41
42
43
44
45
46
47
48
49
50
51
52
53
54
55
56
57
58
59
60

DISCUSSION

1
2
3
4
5
6
7
8 KRAS mutations are routinely detected by allele-specific quantitative PCR, or traditional PCR
9
10 coupled to direct sequencing or pyrosequencing.³⁰ Many PCR-based assays for mutant allele
11
12 discrimination have been described, as it seems convenient to combine the target amplification step
13
14 with the discrimination of the mutation.³¹⁻³⁵ However, most of these methods require additional
15
16 processing steps (restriction enzyme digestions, nested PCR, melting curve analysis), stringent
17
18 hybridization conditions, and often specific instrumentation (HPLC, laser scanners, mass
19
20 spectrometry, real-time PCR devices, fluorometers, capillary gel electrophoresis, luminometers,
21
22 *etc.*) for the readout of the result, reducing simplicity and increasing costs, which is not desirable
23
24
25
26
27 when thinking to a method for fast and large scale population screening.

28
29 In our study, the target amplification is isothermal, thus considerably simpler when compared
30
31 to traditional PCR or real-time PCR, as it can be performed without dedicated instrumentation, by
32
33 simply keeping the temperature at c.a. 65 °C for two hours. Among the different isothermal
34
35 amplification techniques reported in literature, we chose HDA. HDA was particularly suitable for
36
37 our system, as it does not require post-amplification processing steps, it can directly amplify a
38
39 complex template such as human genomic DNA, and it has an optimal target length (around 100
40
41 nt) in a favorable range for a sandwich hybridization. Notably, this isothermal target amplification
42
43 step is not involved in the mutation discrimination, which is performed in the colorimetric
44
45 detection step. Moreover, the volume of amplified product required for the subsequent
46
47 hybridization step is just 3 μ l, which makes the assay potentially adaptable to a microfluidic
48
49 platform for point-of-care applications. In the following detection step, discrimination by naked-
50
51 eye of a single mutation (35G>A) in KRAS gene is achieved at room temperature, in less than two
52
53 hours and under non stringent conditions, using magnetic microparticles and DNA-conjugated
54
55
56
57
58
59
60

1
2
3 AuNPs, reaching a very low limit of detection (20 pM). The combination of different factors
4
5 contributes to the high sensitivity of this method: 1) short discriminating probes enable the
6
7 discrimination of a point mutation at room temperature; 2) cooperative hybridization of two probes
8
9 confers enhanced binding stability to the perfectly matched probe-target duplex at the assay
10
11 conditions; 3) AuNPs probes (40 nm) enhance the visual color detection; 4) signal enhancement on
12
13 the surface of paramagnetic microparticles increase the naked-eye discrimination of the different
14
15 colors, even when starting from diluted samples.
16
17
18

19
20 Several colorimetric methods exploited the distance-dependent color change caused by AuNPs
21
22 aggregation upon recognition of a target nucleic acid. Mirkin's group first demonstrated a
23
24 colorimetric detection scheme based on AuNPs aggregation to achieve single mismatch
25
26 discrimination. The concentration of the synthetic target tested in this proof-of-concept experiment
27
28 was of 60 nM.¹⁸ Thereafter, many group exploited the same principle, to achieve naked-eye
29
30 discrimination of single or multiple point mutations. The simpler schemes based on nanoparticle
31
32 aggregation only reached sensitivities in the nanomolar range.^{10, 36-39} Other reports introduced an
33
34 extra step of melting curve analysis, to improve sensitivity in the mismatch discrimination.⁴⁰ Our
35
36 method for single mismatch discrimination reaches high sensitivity, approaching that of studies
37
38 where multiple mismatches or a fully non-complementary sequence was discriminated from a wt
39
40 target.^{41,42}
41
42
43
44

45
46 Diverse works reported the enzymatic colorimetric discrimination of point mutations or single
47
48 nucleotide polymorphisms. However, simpler methods are often proof-of-principle studies, with
49
50 low sensitivity. On the other hand, many studies applied on real clinical samples required sample
51
52 processing steps employing dedicated instrumentations, or strict control of the hybridization
53
54 stringency conditions. Ausch *et al.*, for instance, detected KRAS mutation in cancer tissue samples
55
56 using mutant enriched PCR, array hybridization, and an enzymatic system for colorimetric
57
58
59
60

1
2
3 readout.⁴³ In this case, standard hybridization required stringency wash and strict temperature
4 control, which are not necessary in our settings, thanks to the use of AuNP-probes and to a probe
5 design which exploits short oligonucleotide probes and enhanced stability through cooperative
6 hybridization of adjacent probes. Other studies avoided the stringency hybridization conditions
7 necessary for the discrimination of a point mutation by coupling a ligation step to AuNP
8 aggregation.²¹ When ligase was used in a PCR-like fashion, with the ligation chain reaction (LCR),
9 it also allowed reaching high sensitivity.⁴⁴ Unfortunately, LCR requires thermal cycles, simplified
10 but conceptually similar to a traditional PCR, which we chose to avoid, in view of low-cost point-
11 of-care applications.
12
13
14
15
16
17
18
19
20
21
22
23

24 Our system uses paramagnetic microbeads to enhance the colorimetric signal of the AuNPs.
25 Other authors have exploited, previously, a combination of microbeads and AuNPs for the
26 colorimetric detection of the presence of a synthetic DNA target⁴⁵ or the discrimination of a two-
27 bases mismatch.⁴⁶ However, the discrimination of a single base mismatch was not attempted in
28 these studies.
29
30
31
32
33
34
35

36 In most of the reports employing AuNP-conjugated DNA probes, DNA sequence specific for
37 the target of interest are conjugated to the AuNPs. Therefore, for each new target, a specific
38 functionalized nanoparticle has to be prepared. One of the advantages of our system is the use of
39 universal poly-T AuNP-probes, which make our assay quickly adaptable to any target, by simply
40 designing a new discriminating sandwich probe. This is much cheaper than preparing new
41 functionalized AuNPs for each target and simplifies multiplexing applications. A previous work by
42 Wilson's group obtained a colorimetric detection based on universal AuNP-probes by conjugating
43 an intercalating agent to AuNPs, and could identify 25 picomol of target DNA.⁴⁷ In comparison,
44 our assay is significantly more sensitive, as it can detect down to 32 fmol of DNA.
45
46
47
48
49
50
51
52
53
54
55
56
57
58
59
60

CONCLUSIONS

Our colorimetric assay is up to 4 orders of magnitude more sensitive than other as-simple AuNPs based colorimetric assays for single mismatch discrimination.^{10, 36-39} The complete assay, from isothermal target amplification to colorimetric readout of the presence or absence of the single base mismatch, can be performed without costly instrumentation, requiring only a very simple heating device. Moreover, very small sample volumes are needed, so that the assay is easily adaptable to lab-on-chip platforms for point-of-care diagnostics, currently under development at our lab. Finally, the assay employs universal detection probes and can thus be easily adapted to multiplexed genotyping of KRAS or to other relevant diagnostic targets. For instance, a small panel of mutations can be screened simultaneously, by hybridizing the amplified gene with different discriminating probes, each specific for a given mutation. Upon hybridization with the universal AuNP probe, a red coloration of the sample would indicate the presence of a specific mutation, which can quickly give an indication of the disease progression and help therapeutic decisions.

The sensitivity of the assay could be further improved by introducing a metal enhancement step,⁴⁸ which might allow the direct colorimetric genotyping of un-amplified genomic DNA samples, as also demonstrated by other authors on array hybridization.^{49,50}

MATERIALS AND METHODS

Synthesis of 40 nm gold nanoparticles

40 nm citrate capped AuNPs were prepared as previously reported.⁵¹ The obtained AuNPs were characterized by UV-vis spectrophotometry, DLS, TEM and SEM (Supporting Information, **Figure S4**).

Conjugation of AuNPs with DNA probes

AuNPs-conjugated DNA probes were prepared according to published protocols.⁵²⁻⁵⁴ Briefly, thiolated probe oligonucleotides ($T_{(30)}-(O-CH_2-CH_2)_3-SH$), purchased from IDT DNA, were digested with 10 mM Tris(2-carboxyethyl)phosphine (TCEP) for 3 hours at room temperature. The digested oligonucleotides were then incubated with 40 nm AuNPs in a 2000:1 molar ratio overnight, at room temperature, under mild shaking. The AuNPs-DNA mixture was then brought to 0.3 M NaCl in 10 mM phosphate buffer, pH 7.4, 0.01% SDS, with stepwise increment of salt over the course of 8 hours. After an additional overnight incubation at room temperature, the DNA-conjugated AuNPs were centrifuged and washed with 0.3 M NaCl in 10 mM phosphate buffer plus 0.01% SDS, in order to remove the excess unbound DNA. These probes were stored at 4 °C until their use. To determine the density of DNA probes on the nanoparticle surface, 10 μ l of these DNA-conjugated AuNPs were digested overnight with 1 mM DTT in 90 mM phosphate buffer, pH 8, at 40 °C. The mixture was centrifuged at 13,400 rpm for 15 min in a bench-top centrifuge, and the amount of oligonucleotides in the supernatant was estimated using the Quant-iT™ OliGreen® ssDNA Kit (Invitrogen). The concentration of AuNPs was measured by UV-vis spectroscopy and Inductively Coupled Plasma – Atomic Emission Spectroscopy (ICP-AES). On average, 686 ± 64 copies of probe oligonucleotide were found to be linked to each nanoparticle.

Cell lines and control of KRAS status

The cell lines used were obtained from American Type Culture Collection (Manassas, VA). HT-29 cells were maintained at 37°C with 5% CO₂ and cultured in McCoy's 5A (Invitrogen) supplemented with 10% FBS. LS180 cell lines were cultured in Eagle's Minimum Essential Medium (Gibco, NY, USA) supplemented with 10% fetal bovine serum. Cells were tested and authenticated using the StemElite ID System (Promega). Mutational analysis of KRAS was done as previously described⁵⁵ using primers amplifying codon 12 of the gene.

Extraction of genomic DNA from cell cultures

Genomic DNA was extracted from cultured cell lines HT29 (wt) and LS180 (heterozygous for mutation 35G>A) using DNeasy Blood & Tissue Kit (Qiagen). The concentration and purity of extracted DNA was measured using a UV spectrophotometer.

PCR and Helicase Dependent Amplification

A 101 bp fragment including codons 12 and 13 in KRAS was amplified from genomic DNA using either a traditional PCR or a two-step isothermal amplification with the IsoAmp® II Universal tHDA Kit (Biohelix). Briefly, for PCR, reaction mixtures contained 100 ng genomic DNA, 75 nM FW primer, 75 nM biotinylated REV primer, 2.5 mM MgCl₂, 1X PCR reaction buffer, 0.5 µl HotStart Taq (EuroClone). Thermal cycles were as follow: 15' at 95 °C, followed by 30 cycles of 94 °C (1'), 55 °C (1'), 72 °C (1'), and a final extension step of 10' at 72 °C.

For HDA, 200 ng of template genomic DNA was denaturated for 5 min at 95 °C in the annealing buffer of the kit plus 75 nM FW primer and 75 nM biotinylated REV primer. The mixture was then placed on ice and a reaction mix containing 3.5 µl of IsoAmp® Enzyme Mix, 3.5 µl of IsoAmp® dNTP Solution, 40 mM NaCl and 4 mM MgSO₄ in annealing buffer was added. This mixture was then incubated at 65 °C for 2 hours. A 5 µl aliquot of the reaction was

1
2
3 electrophoresed on a 2% agarose gel in 0.5% TBE to verify the presence of the desired amplicon
4
5 and the absence of unspecific amplification.
6
7

8 *Hybridization and colorimetric detection of single mismatch*

9

10 5 μl of Dynabeads® M-280 Streptavidin (Invitrogen) paramagnetic beads were washed twice
11 with hybridization buffer (HB) (1X PBS pH 7.4 plus 5% w/v PEG 600), resuspended in an equal
12 volume of HB and incubated with varying amount of biotinylated PCR or HDA product for 20 min
13 at room temperature. The beads were then incubated with 0.15 M NaOH for 5 min, to denature
14 the double strand amplification product and magnetically separate the interfering non-biotinylated
15 strand. The beads were subsequently washed with 100 μl 0.15 M NaOH and then with 100 μl HB,
16 then resuspended in 20 μl of HB. 100 pmol of probe, recognizing the wt or point mutated target,
17 were added to the beads and incubated for 10 minutes at room temperature, then 100 fmol of
18 DNA-conjugated AuNPs were added and incubated for 1 hour at room temperature. The mixture
19 was then washed three times with HB and the color readout ascertained visually. The UV-vis
20 spectrum was also measured.
21
22
23
24
25
26
27
28
29
30
31
32
33
34
35

36 In experiments aimed at assessing the contribution of cooperative hybridization, the
37 discriminating probe and the detection probe were either allowed to hybridize at the same time
38 with the target, or they were hybridized sequentially. In this latter case, the discriminating probe
39 was added alone for one hour, after which it was removed by magnetic separation. Then, after a
40 washing step, the AuNP-conjugated detection probe was added and it was incubated with the beads
41 for one extra hour. The sequences of all probes and primers used in this study are reported in Table
42
43
44
45
46
47
48
49
50
51 1.

52 *ICP-AES analysis*

53

54
55 After the hybridization, 10 μl of each sample, containing wt or mutant target were digested
56 overnight with 500 μl of aqua regia (1 part of nitric acid and 3 parts of hydrochloric acid). The
57
58
59
60

1
2
3 next day, the mixture was diluted 100 times and ICP-AES analysis was performed using two
4
5 different standard curves, one for gold and one for iron. The gold content in the two samples, as
6
7 resulting from the analysis, was normalized for the iron amount in each of them, in order to avoid
8
9 mistakes that might arise by any possible dis-homogeneity during sampling from the beads
10
11 suspension.
12
13

14
15
16
17 **Acknowledgments:** This work was partially supported by the Italian Flagship Project NanoMax.
18
19

20
21
22 **Supporting Information Available:** Additional graphical data and images as described in the text.
23

24 This material is available free of charge *via* the Internet at <http://pubs.acs.org>.
25
26
27
28
29
30
31
32
33
34
35
36
37
38
39
40
41
42
43
44
45
46
47
48
49
50
51
52
53
54
55
56
57
58
59
60

REFERENCES

- 1 Arrington, A. K.; Heinrich, E. L.; Lee, W.; Duldulao, M.; Patel, S.; Sanchez, J.; Garcia-Aguilar, J.; Kim, J. Prognostic and Predictive Roles of Kras Mutation in Colorectal Cancer. *Int. J. Mol. Sci.* **2012**, *10*, 12153-12168.
- 2 Adjei, A. A. Blocking Oncogenic Ras Signaling for Cancer Therapy. *J. Natl. Cancer Inst.* **2001**, *14*, 1062-1074.
- 3 Neumann, J.; Zeindl-Eberhart, E.; Kirchner, T.; Jung, A. Frequency and Type of Kras Mutations in Routine Diagnostic Analysis of Metastatic Colorectal Cancer. *Pathol. Res. Pract.* **2009**, *12*, 858-862.
- 4 Nash, G. M.; Gimbel, M.; Shia, J.; Nathanson, D. R.; Ndubuisi, M. I.; Zeng, Z. S.; Kemeny, N.; Paty, P. B. Kras Mutation Correlates with Accelerated Metastatic Progression in Patients with Colorectal Liver Metastases. *Ann. Surg. Oncol.* **2010**, *2*, 572-578.
- 5 Allegra, C. J.; Jessup, J. M.; Somerfield, M. R.; Hamilton, S. R.; Hammond, E. H.; Hayes, D. F.; McAllister, P. K.; Morton, R. F.; Schilsky, R. L. American Society of Clinical Oncology Provisional Clinical Opinion: Testing for Kras Gene Mutations in Patients with Metastatic Colorectal Carcinoma to Predict Response to Anti-Epidermal Growth Factor Receptor Monoclonal Antibody Therapy. *J. Clin. Oncol.* **2009**, *12*, 2091-2096.
- 6 Domagala, P.; Hybiak, J.; Sulzyc-Bielicka, V.; Cybulski, C.; Rys, J.; Domagala, W. Kras Mutation Testing in Colorectal Cancer as an Example of the Pathologist's Role in Personalized Targeted Therapy: A Practical Approach. *Pol. J. Pathol.* **2012**, *3*, 145-164.
- 7 Bichenkova, E. V.; Lang, Z.; Yu, X.; Rogert, C.; Douglas, K. T. DNA-Mounted Self-Assembly: New Approaches for Genomic Analysis and Snp Detection. *Biochim. Biophys. Acta* **2011**, *1*, 1-23.
- 8 Hardenbol, P.; Yu, F.; Belmont, J.; Mackenzie, J.; Bruckner, C.; Brundage, T.; Boudreau, A.; Chow, S.; Eberle, J.; Erbilgin, A., *et al.* Highly Multiplexed Molecular Inversion Probe Genotyping: Over 10,000 Targeted Snps Genotyped in a Single Tube Assay. *Genome Res.* **2005**, *2*, 269-275.
- 9 Olivier, M.; Chuang, L. M.; Chang, M. S.; Chen, Y. T.; Pei, D.; Ranade, K.; de Witte, A.; Allen, J.; Tran, N.; Curb, D., *et al.* High-Throughput Genotyping of Single Nucleotide Polymorphisms Using New Biplex Invader Technology. *Nucleic Acids Res.* **2002**, *30*, e53.
- 10 Chen, Y. T.; Hsu, C. L.; Hou, S. Y. Detection of Single-Nucleotide Polymorphisms Using Gold Nanoparticles and Single-Strand-Specific Nucleases. *Anal. Biochem.* **2008**, *2*, 299-305.
- 11 Mohammed, M. I.; Sills, G. J.; Brodie, M. J.; Ellis, E. M.; Girkin, J. M. A Complete Miniaturised Genotyping System for the Detection of Single Nucleotide Polymorphisms in Human DNA Samples. *Sens. Actuators B* **2009**, *1*, 83-90.
- 12 Kreibig, U.; Genzel, L. Optical Absorption of Small Metallic Particles. *Surf. Sci.* **1985**, *156*, 678-700.
- 13 Grabar, K. C.; Smith, P. C.; Musick, M. D.; Davis, J. A.; Walter, D. G.; Jackson, M. A.; Guthrie, A. P.; Natan, M. J. Kinetic Control of Interparticle Spacing in Au Colloid-Based Surfaces: Rational Nanometer-Scale Architecture. *J. Am. Chem. Soc.* **1996**, *5*, 1148-1153.
- 14 Giljohann, D. A.; Seferos, D. S.; Daniel, W. L.; Massich, M. D.; Patel, P. C.; Mirkin, C. A. Gold Nanoparticles for Biology and Medicine. *Angew. Chem. Int. Ed.* **2010**, *19*, 3280-3294.
- 15 Dreaden, E. C.; Alkilany, A. M.; Huang, X.; Murphy, C. J.; El-Sayed, M. A. The Golden Age: Gold Nanoparticles for Biomedicine. *Chem. Soc. Rev.* **2012**, *7*, 2740-2779.
- 16 Orendorff, C. J.; Sau, T. K.; Murphy, C. J. Shape-Dependent Plasmon-Resonant Gold Nanoparticles. *Small* **2006**, *5*, 636-639.
- 17 Carregal-Romero, S.; Montenegro, J. M.; Parak, W. J.; Rivera Gil, P. Subcellular Carrier-Based Optical Ion-Selective Nanosensors. *Front. Neuropharmacol.* **2012**, *70*, 1-7.

- 1
2
3 18 Storhoff, J. J.; Elghanian, R.; Mucic, R. C.; Mirkin, C. A.; Letsinger, R. L. One-Pot Colorimetric
4 Differentiation of Polynucleotides with Single Base Imperfections Using Gold Nanoparticle Probes. *J.*
5 *Am. Chem. Soc.* **1998**, *9*, 1959-1964.
6
7 19 Reynolds, R. A.; Mirkin, C. A.; Letsinger, R. L. Homogeneous, Nanoparticle-Based Quantitative
8 Colorimetric Detection of Oligonucleotides. *J. Am. Chem. Soc.* **2000**, *15*, 3795-3796.
9
10 20 Storhoff, J. J.; Lucas, A. D.; Garimella, V.; Bao, Y. P.; Muller, U. R. Homogeneous Detection of
11 Unamplified Genomic DNA Sequences Based on Colorimetric Scatter of Gold Nanoparticle Probes.
12 *Nat. Biotechnol.* **2004**, *7*, 883-887.
13
14 21 Li, J.; Chu, X.; Liu, Y.; Jiang, J. H.; He, Z.; Zhang, Z.; Shen, G.; Yu, R. Q. A Colorimetric Method for
15 Point Mutation Detection Using High-Fidelity DNA Ligase. *Nucleic Acids Res.* **2005**, *33*, e168.
16
17 22 Oh, J. H.; Lee, J. S. Designed Hybridization Properties of DNA-Gold Nanoparticle Conjugates for the
18 Ultrasensitive Detection of a Single-Base Mutation in the Breast Cancer Gene *Brcal*. *Anal. Chem.*
19 **2011**, *19*, 7364-7370.
20
21 23 de la Rica, R.; Stevens, M. M. Plasmonic Elisa for the Ultrasensitive Detection of Disease Biomarkers
22 with the Naked Eye. *Nat. Nanotechnol.* **2012**, *12*, 821-824.
23
24 24 Lee, H.; Joo, S. W.; Lee, S. Y.; Lee, C. H.; Yoon, K. A.; Lee, K. Colorimetric Genotyping of Single
25 Nucleotide Polymorphism Based on Selective Aggregation of Unmodified Gold Nanoparticles.
26 *Biosens. Bioelectron.* **2010**, *2*, 730-735.
27
28 25 Qi, Y.; Li, B. A Sensitive, Label-Free, Aptamer-Based Biosensor Using a Gold Nanoparticle-Initiated
29 Chemiluminescence System. *Chemistry* **2011**, *5*, 1642-1648.
30
31 26 Zhang, D. Y. Cooperative Hybridization of Oligonucleotides. *J. Am. Chem. Soc.* **2010**, *4*, 1077-1086.
32
33 27 Lane, M. J.; Paner, T.; Kashin, I.; Faldasz, B. D.; Li, B.; Gallo, F. J.; Benight, A. S. The
34 Thermodynamic Advantage of DNA Oligonucleotide 'Stacking Hybridization' Reactions: Energetics of
35 a DNA Nick. *Nucleic Acids Res.* **1997**, *3*, 611-617.
36
37 28 Jin, R.; Wu, G.; Li, Z.; Mirkin, C. A.; Schatz, G. C. What Controls the Melting Properties of DNA-
38 Linked Gold Nanoparticle Assemblies? *J. Am. Chem. Soc.* **2003**, *6*, 1643-1654.
39
40 29 Vincent, M.; Xu, Y.; Kong, H. Helicase-Dependent Isothermal DNA Amplification. *EMBO Rep.* **2004**,
41 *8*, 795-800.
42
43 30 Dufort, S.; Richard, M. J.; de Fraipont, F. Pyrosequencing Method to Detect *Kras* Mutation in
44 Formalin-Fixed and Paraffin-Embedded Tumor Tissues. *Anal. Biochem.* **2009**, *2*, 166-168.
45
46 31 Levi, S.; Urbano-Ispizua, A.; Gill, R.; Thomas, D. M.; Gilbertson, J.; Foster, C.; Marshall, C. J.
47 Multiple *K-Ras* Codon 12 Mutations in Cholangiocarcinomas Demonstrated with a Sensitive
48 Polymerase Chain Reaction Technique. *Cancer Res.* **1991**, *13*, 3497-3502.
49
50 32 Clayton, S. J.; Scott, F. M.; Walker, J.; Callaghan, K.; Haque, K.; Liloglou, T.; Xinarianos, G.;
51 Shawcross, S.; Ceuppens, P.; Field, J. K., *et al.* *K-Ras* Point Mutation Detection in Lung Cancer:
52 Comparison of Two Approaches to Somatic Mutation Detection Using Arms Allele-Specific
53 Amplification. *Clin. Chem.* **2000**, *12*, 1929-1938.
54
55 33 Behn, M.; Thiede, C.; Neubauer, A.; Pankow, W.; Schuermann, M. Facilitated Detection of Oncogene
56 Mutations from Exfoliated Tissue Material by a Pna-Mediated 'Enriched Pcr' Protocol. *J. Pathol.* **2000**,
57 *1*, 69-75.
58
59 34 Luo, J. D.; Chan, E. C.; Shih, C. L.; Chen, T. L.; Liang, Y.; Hwang, T. L.; Chiou, C. C. Detection of
60 Rare Mutant *K-Ras* DNA in a Single-Tube Reaction Using Peptide Nucleic Acid as Both Pcr Clamp
and Sensor Probe. *Nucleic Acids Res.* **2006**, *34*, e12.

- 1
2
3 35 Kriegshauser, G.; Fabjani, G.; Ziegler, B.; Zochbauer-Muller, S.; End, A.; Zeillinger, R. Biochip-Based
4 Detection of Kras Mutation in Non-Small Cell Lung Cancer. *Int. J. Mol. Sci.* **2011**, 12, 8530-8538.
- 5
6 36 Taton, T. A.; Lu, G.; Mirkin, C. A. Two-Color Labeling of Oligonucleotide Arrays *Via* Size-Selective
7 Scattering of Nanoparticle Probes. *J. Am. Chem. Soc.* **2001**, 21, 5164-5165.
- 8
9 37 Li, H.; Rothberg, L. Colorimetric Detection of DNA Sequences Based on Electrostatic Interactions
10 with Unmodified Gold Nanoparticles. *Proc. Natl. Acad. Sci. U. S. A.* **2004**, 39, 14036-14039.
- 11
12 38 Murphy, D.; O'Brien, P.; Redmond, G. Sub-Picomole Colorimetric Single Nucleotide Polymorphism
13 Discrimination Using Oligonucleotide-Nanoparticle Conjugates. *Analyst* **2004**, 10, 970-974.
- 14
15 39 Charrier, A.; Candoni, N.; Liachenko, N.; Thibaudau, F. 2d Aggregation and Selective Desorption of
16 Nanoparticle Probes: A New Method to Probe DNA Mismatches and Damages. *Biosens. Bioelectron.*
17 **2007**, 22, 1881-1886.
- 18
19 40 Li, J.; Jiang, J. H.; Xu, X. M.; Chu, X.; Jiang, C.; Shen, G.; Yu, R. Q. Simultaneous Identification of
20 Point Mutations *Via* DNA Ligase-Mediated Gold Nanoparticle Assembly. *Analyst* **2008**, 7, 939-945.
- 21
22 41 Xia, F.; Zuo, X.; Yang, R.; Xiao, Y.; Kang, D.; Vallee-Belisle, A.; Gong, X.; Yuen, J. D.; Hsu, B. B.;
23 Heeger, A. J., *et al.* Colorimetric Detection of DNA, Small Molecules, Proteins, and Ions Using
24 Unmodified Gold Nanoparticles and Conjugated Polyelectrolytes. *Proc. Natl. Acad. Sci. U. S. A.* **2010**,
25 24, 10837-10841.
- 26
27 42 Cordray, M. S.; Amdahl, M.; Richards-Kortum, R. R. Gold Nanoparticle Aggregation for
28 Quantification of Oligonucleotides: Optimization and Increased Dynamic Range. *Anal. Biochem.* **2012**,
29 2, 99-105.
- 30
31 43 Ausch, C.; Buxhofer-Ausch, V.; Oberkanins, C.; Holzer, B.; Minai-Pour, M.; Jahn, S.; Dandachi, N.;
32 Zeillinger, R.; Kriegshauser, G. Sensitive Detection of Kras Mutations in Archived Formalin-Fixed
33 Paraffin-Embedded Tissue Using Mutant-Enriched Pcr and Reverse-Hybridization. *J. Mol. Diagn.*
34 **2009**, 6, 508-513.
- 35
36 44 Shen, W.; Deng, H.; Gao, Z. Gold Nanoparticle-Enabled Real-Time Ligation Chain Reaction for
37 Ultrasensitive Detection of DNA. *J. Am. Chem. Soc.* **2012**, 36, 14678-14681.
- 38
39 45 Reynolds, R. A.; Mirkin, C. A.; Letsinger, R. L. A Gold Nanoparticle/Latex Microsphere-Based
40 Colorimetric Oligonucleotide Detection Method. *Pure Appl. Chem.* **2000**, 72, 229-235.
- 41
42 46 Chen, Y.; Aveyard, J.; Wilson, R. Gold and Silver Nanoparticles Functionalized with Known Numbers
43 of Oligonucleotides Per Particle for DNA Detection. *Chem. Commun.* **2004**, 24, 2804-2805.
- 44
45 47 Mehrabi, M.; Wilson, R. Intercalating Gold Nanoparticles as Universal Labels for DNA Detection.
46 *Small* **2007**, 9, 1491-1495.
- 47
48 48 Taton, T. A.; Mirkin, C. A.; Letsinger, R. L. Scanometric DNA Array Detection with Nanoparticle
49 Probes. *Science* **2000**, 289, 1757-1760.
- 50
51 49 Storhoff, J. J.; Marla, S. S.; Bao, P.; Hagenow, S.; Mehta, H.; Lucas, A.; Garimella, V.; Patno, T.;
52 Buckingham, W.; Cork, W., *et al.* Gold Nanoparticle-Based Detection of Genomic DNA Targets on
53 Microarrays Using a Novel Optical Detection System. *Biosens. Bioelectron.* **2004**, 8, 875-883.
- 54
55 50 Bao, Y. P.; Huber, M.; Wei, T. F.; Marla, S. S.; Storhoff, J. J.; Muller, U. R. Snp Identification in
56 Unamplified Human Genomic DNA with Gold Nanoparticle Probes. *Nucleic Acids Res.* **2005**, 33, e15.
- 57
58 51 Pompa, P. P.; Vecchio, G.; Galeone, A.; Brunetti, V.; Maiorano, G.; Sabella, S.; Cingolani, R. Physical
59 Assessment of Toxicology at Nanoscale: Nano Dose-Metrics and Toxicity Factor. *Nanoscale* **2011**, 7,
60 2889-2897.
- 52 Mirkin, C. A.; Letsinger, R. L.; Mucic, R. C.; Storhoff, J. J. A DNA-Based Method for Rationally
Assembling Nanoparticles into Macroscopic Materials. *Nature* **1996**, 382, 607-609.

- 1
2
3 53 Hurst, S. J.; Lytton-Jean, A. K.; Mirkin, C. A. Maximizing DNA Loading on a Range of Gold
4 Nanoparticle Sizes. *Anal. Chem.* **2006**, 24, 8313-8318.
5
6 54 Alhasan, A. H.; Kim, D. Y.; Daniel, W. L.; Watson, E.; Meeks, J. J.; Thaxton, C. S.; Mirkin, C. A.
7 Scanometric MicroRNA Array Profiling of Prostate Cancer Markers Using Spherical Nucleic Acid-Gold
8 Nanoparticle Conjugates. *Anal. Chem.* **2012**, 9, 4153-4160.
9
10 55 Reid, J. F.; Gariboldi, M.; Sokolova, V.; Capobianco, P.; Lampis, A.; Perrone, F.; Signoroni, S.; Costa,
11 A.; Leo, E.; Pilotti, S., *et al.* Integrative Approach for Prioritizing Cancer Genes in Sporadic Colon
12 Cancer. *Genes Chromosomes Cancer* **2009**, 11, 953-962.
13
14
15
16
17
18
19
20
21
22
23
24
25
26
27
28
29
30
31
32
33
34
35
36
37
38
39
40
41
42
43
44
45
46
47
48
49
50
51
52
53
54
55
56
57
58
59
60

Table 1. Sequence of probes and primers (the position of the point mutation is underlined).

Name	Sequence	Function
Probe wt	5'AGCTG <u>G</u> TGGCGTAGGpoly(A) ₃₀ 3'	discriminating probe
Probe 35G>A	5'AGCTG <u>A</u> TGGCGTAGGpoly(A) ₃₀ 3'	discriminating probe
FW primer	5'AGGCCTGCTGAAAATGACTGAA3'	primer
REV primer	5'Biotin-CCACAAAATGATTCTGAATTAGCTGTA3'	primer
AuNP probe	5'SH-(O-CH ₂ -CH ₂) ₃ -T ₍₃₀₎ 3'	detection probe

1
2
3
4
5
6
7
8
9
10
11
12
13
14
15
16
17
18
19
20
21
22
23
24
25
26
27
28
29
30
31
32
33
34
35
36
37
38
39
40
41
42
43
44
45
46
47
48
49
50
51
52
53
54
55
56
57
58
59
60

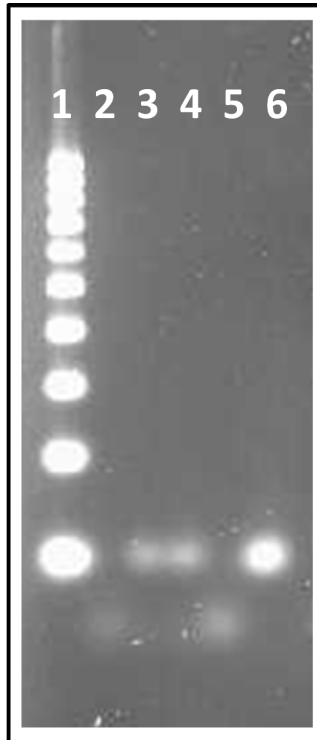


Figure 1. Isothermal amplification of KRAS target. Lane 1: 1Kb marker; Lanes 2 and 5: negative controls; Lanes 3 and 4: 101bp amplified KRAS target; lane 6: internal positive control of the kit.

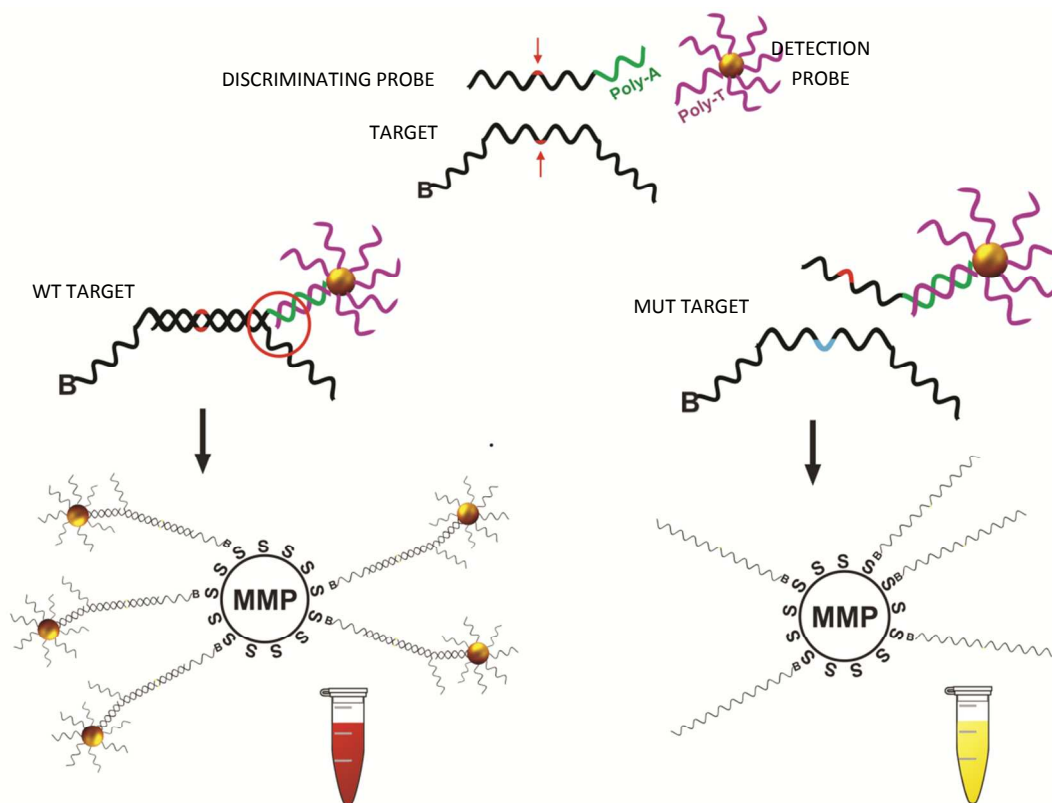


Figure 2. Reaction scheme of the KRAS genotyping assay. When discriminating probe and target are perfectly matched (left), the probe binds both the biotinylated target with its 5' portion and the AuNP probe with its poly(A) 3' portion, and cooperative binding stabilizes the hybrid (red circle). This complex, captured by the streptavidinated paramagnetic beads, gives a red color to the suspension, thanks to the presence of the AuNPs. On the other side (right), a point mutation in the target (light blue) impairs the proper hybridization of the probe with the target, so that the AuNP-probes are washed away during magnetic separation, resulting in a background yellow color (due to the magnetic beads). Abbreviations: MMP= Paramagnetic Microparticle; S=Streptavidin; B=Biotin.

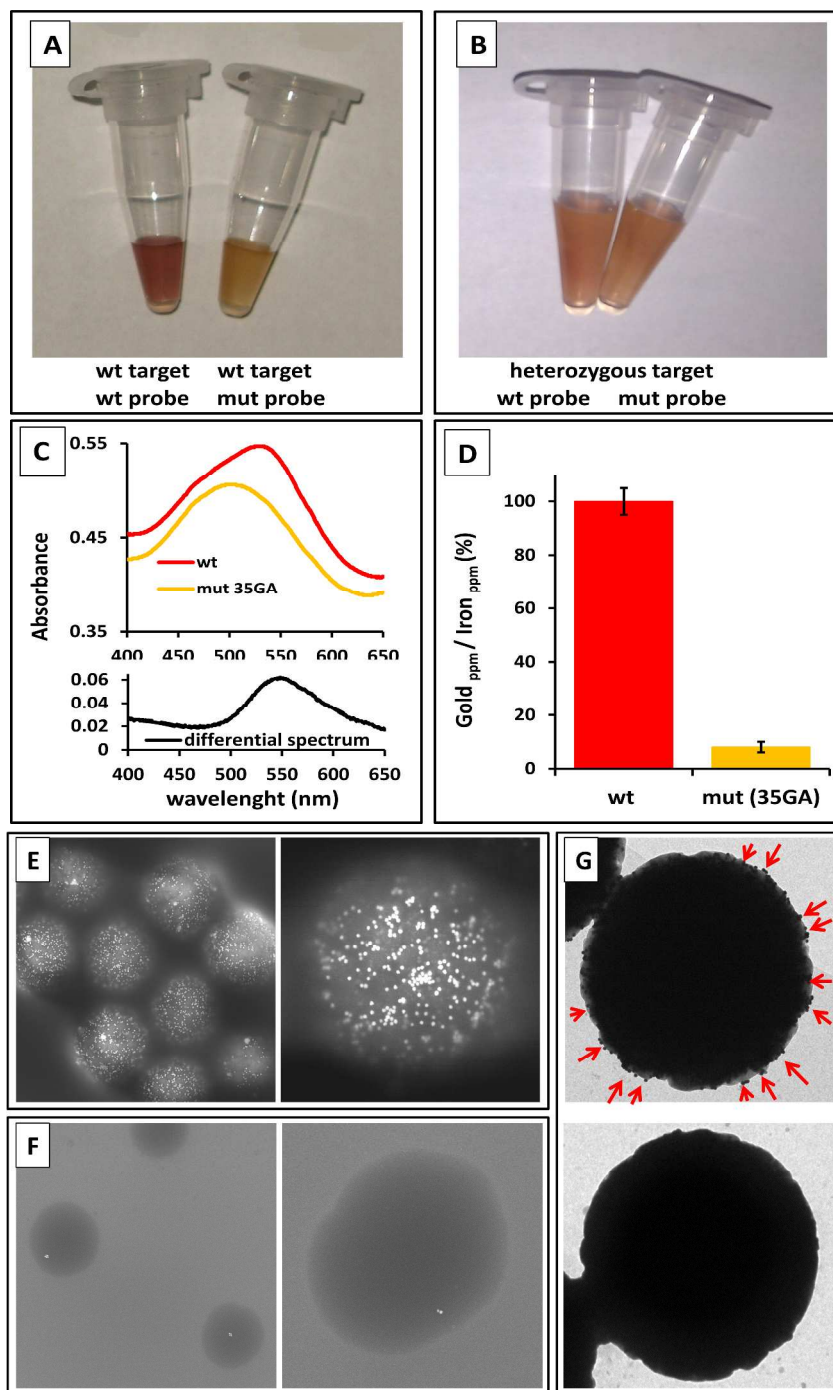


Figure 3. Discrimination of the cancer-related mutation 35G>A in KRAS. (A) naked eye discrimination of point mutation 35G>A; (B) heterozygous cell line hybridizes partially with both wt and mutant probes, giving an intermediate color (orange); (C) UV-vis spectra of wt and mut samples, and differential spectrum (wt minus mut spectra); (D) ICP measurement of gold and iron in samples containing wt or point mutated target; (E) SEM images of the magnetic beads after hybridization with target and AuNP-probes. In samples containing wt target, the magnetic beads are decorated with several AuNPs (brilliant dots); (F) in samples containing point mutated targets, only rare AuNPs bind the magnetic beads. (G) TEM images of samples containing wt type target (upper picture) and point mutated target (lower picture). Arrows highlight AuNP-probes hybridized on matched target on the surface of magnetic beads.

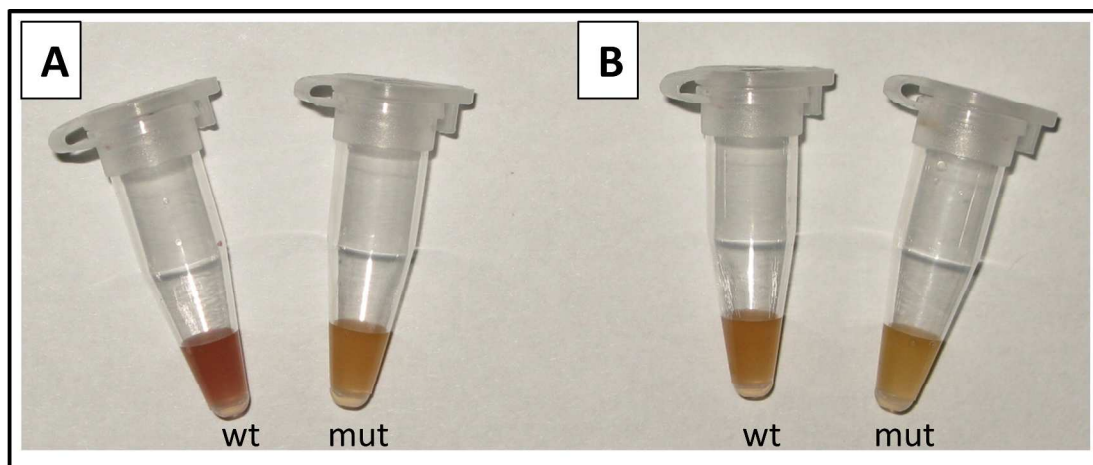
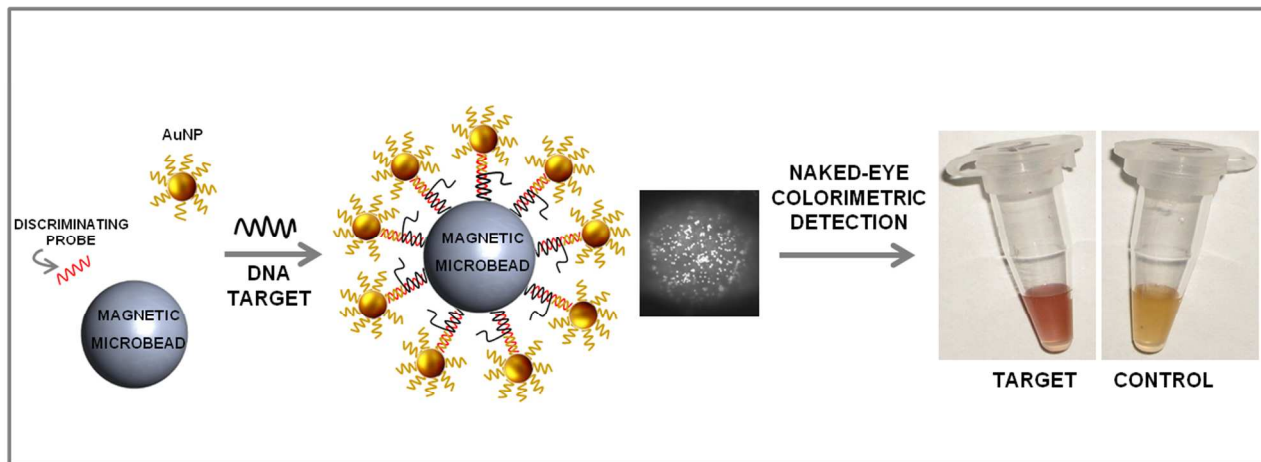


Figure 4. Effect of cooperative hybridization of oligonucleotides. In A, the discriminating probe and the detection probe are allowed to hybridize together and a clear discrimination of the single point mutation is achieved in 70 minutes. In B, the discrimination probes is incubated alone for 1 hour with the target, then, after a washing step, the detection probe is added and incubated for an additional 1 hour, so that parallel cooperative hybridization is not possible. Notwithstanding the longer incubation time, almost no discrimination of the point mutation is achieved in B, indicating that the binding affinity of the first probe alone, at room temperature and in the assay conditions, is not enough to detect the target, and that the enhancement of stability due to cooperative hybridization is necessary for detection.

TOC Graphic



1
2
3
4
5
6
7
8
9
10
11
12
13
14
15
16
17
18
19
20
21
22
23
24
25
26
27
28
29
30
31
32
33
34
35
36
37
38
39
40
41
42
43
44
45
46
47
48
49
50
51
52
53
54
55
56
57
58
59
60